JOC*Article*

Evaluation of the Binding Ability of a Novel Dioxatetraazamacrocyclic Receptor that Contains Two Phenanthroline Units: Selective Uptake of Carboxylate Anions

Carla Cruz,[†] Rita Delgado,[‡,§] Michael G. B. Drew,[||] and Vítor Félix*,[†]

Departamento Química, CICECO, Universidade de Aveiro, 3810-193 Aveiro, Portugal, Instituto de Tecnologia Química e Biológica, UNL, Apartado 127, 2781-901 Oeiras, Portugal, Instituto Superior Técnico, Av. Rovisco Pais, 1049-001 Lisboa, Portugal, and School of Chemistry, University of Reading, Whiteknights, Reading RG6 6AD, United Kingdom

vfelix@dq.ua.pt

Received December 25, 2006

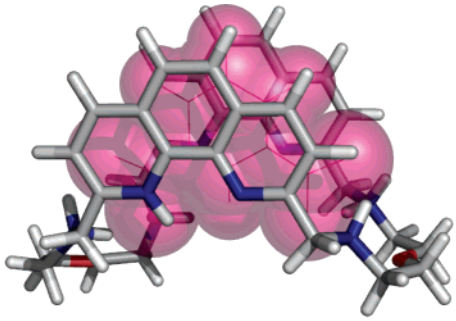

The novel dioxatetraaza macrocycle [26]phen$_2$N$_4$O$_2$, which incorporates two phenanthroline units, has been synthesized, and its acid−base behavior has been evaluated by potentiometric and ^{1}H NMR methods. Six protonation constants were determined, and the protonation sequence was established by NMR. The location of the fifth proton on the phen nitrogen was confirmed by X-ray determinations of the crystal structures of the receptor as bromide and chloride salts. The two compounds have the general molecular formula $\{(H_5[26]phen_2N_4O_2)X_n(H_2O)_{5-n}\}X_{n-1}\cdot mH_2O$, where X = Cl, n = 3, and m = 6 or X = Br, n = 4, and m = 5.5. In the solid state, the $(H_5[26]phen_2N_4O_2)^{5+}$ cation adopts a "horseshoe" topology with sufficient room to encapsulate three or four halogen anions through the several N−H···X hydrogen-bonding interactions. Two supermolecules $\{(H_5[26]phen_2N_4O_2)X_n(H_2O)_{5-n}\}^{(5-n)+}$ form an interpenetrating dimeric species, which was also found by ESI mass spectrum. Binding studies of the protonated macrocycle with aliphatic (ox^{2-}, mal^{2-}, suc^{2-}, cit^{3-}, cta^{3-}) and aromatic (bzc^-, $naphc^-$, $anthc^-$, $pyrc^-$, ph^{2-}, iph^{2-}, tph^{2-}, btc^{3-}) anions were determined in water by potentiometric methods. These studies were complemented by ^{1}H NMR titrations in D_2O of the receptor with selected anions. The $H_i[26]phen_2N_4O_2^{i+}$ receptor can selectively uptake highly charged or extended aromatic carboxylate anions, such as btc^{3-} and $pyrc^-$, in the pH ranges of 4.0−8.5 and <4.0, respectively, from aqueous solution that contain the remaining anions as pollutants or contaminants. To obtain further insight into these structural and experimental findings, molecular dynamics (MD) simulations were carried out in water solution.

Introduction

Carboxylate substrates participate in many chemical, biological, and environmental processes.[1] A wide number of these compounds are used in several industrial applications.[1] For instance, trimesic acid (1,3,5-benzenetricarboxylic acid) is applied in the manufacture of plastics, fibers, water-soluble resins, etc.; oxalic acid is used by the antibiotic industry as a purifying agent of oxytetracycline and chloramphenicol deriva-

* To whom correspondence should be addressed. Phone: 351 234 370729, fax: 351 234 370084.
[†] Universidade de Aveiro.
[‡] Instituto de Tecnologia Química e Biológica.
[§] Instituto Superior Técnico.
[||] University of Reading.

(1) (a) *Supramolecular Chemistry of Anions*; Bianchi, A.; Bowman-James, K.; García-España, E., Eds.; Wiley−VCH: New York, 1997. (b) Amendola, V.; Bonizzoni, M.; Esteban-Gómez, D.; Fabbrizzi, L.; Licchelli, M.; Sancenón, F.; Taglietti, A. *Coord. Chem. Rev.* **2006**, *250*, 1451−1470.

10.1021/jo062653p CCC: $37.00
Published on Web 04/21/2007

CHART 1. Macrocycle Studied in This Work ([26]phen$_2$N$_4$O$_2$) with Carboxylate Anions

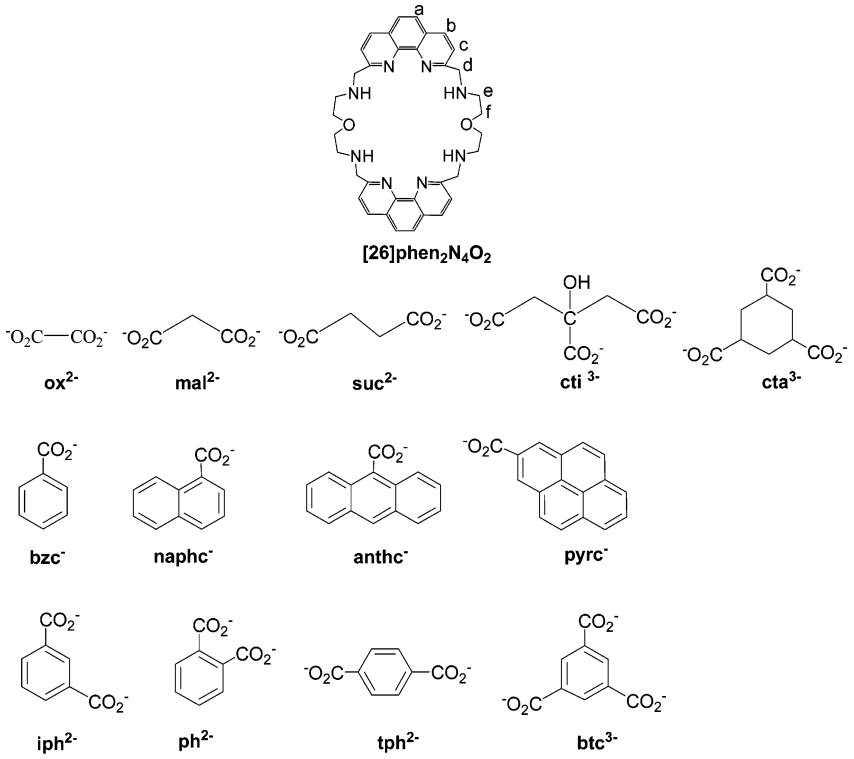

CHART 2. Other Compounds Used for Comparison Reasons

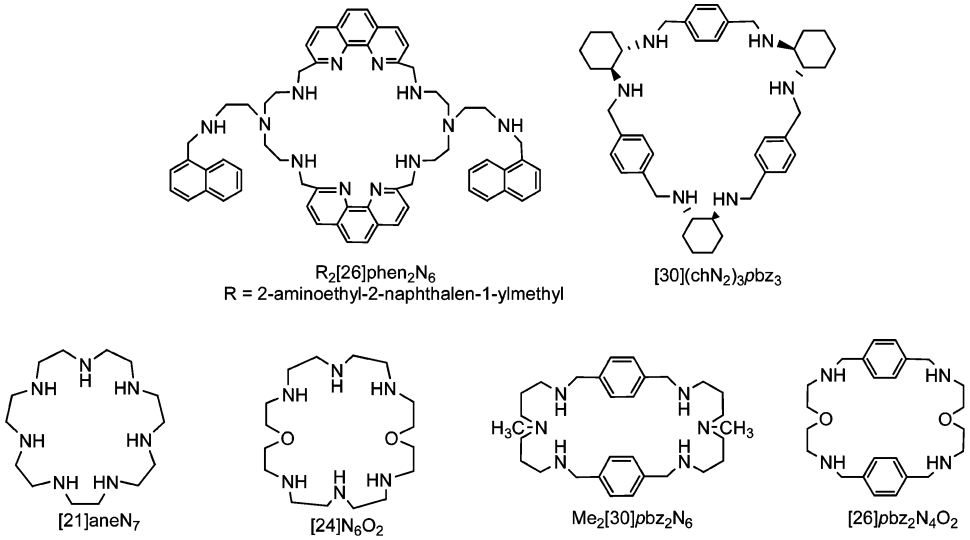

tives; succinic acid is used as an additive in the pharmaceutical and food chemistry industries; phthalic, isophthalic, terephthalic, and benzoic acids are used in the manufacture of paper, cosmetics, plastics, dyes, and paints.[2] On the other hand, polycyclic aromatic hydrocarbons (PAHs), such as anthracene, naphthalene, phenanthrene, pyrene, and their carboxylate derivatives, are ubiquitous contaminants of aquatic environments.[3] Therefore, the sensing of and the selective uptake of this type of substrate are absolutely necessary; nowadays, supramolecular chemists are responding to this challenge with the molecular design and preparation of novel functional synthetic receptors.[4]

In this context, we synthesized the macrocycle [26]phen$_2$N$_4$O$_2$ that is outlined in Chart 1. This receptor incorporates two 1,10-phenathroline (phen) units and has a rigid structure with at least four N−H potential binding sites. In the solid state, its protonated form, $\{H_5[26]phen_2N_4O_2\}^{5+}$, adopts a pre organized cavity with a "horseshoe" shape that is stabilized by multiple N−H···N and N−H···O intramolecular hydrogen bonds that are completed by N−H···Cl (Br) hydrogen-bonding interactions with anions. This result prompted us to envisage the protonated forms of [26]phen$_2$N$_4$O$_2$ as receptors that are capable of promoting the selective uptake of and sensing of aliphatic and

(2) *Chemical Land 21*, http://www.chemicalland21.com.
(3) Potrykus, J.; Albalat, A.; Pempkowiak, J.; Porte, C. *Oceanologia* **2003**, *45*, 337−355.
(4) (a) García-España, E.; Díaz, P.; Llinares, J. M.; Clares, M. P.; Bianchi, A. *Coord. Chem. Rev.* **2006**, *250*, 2952−2986. (b) Gale, P. A.; Quesada, R. *Coord. Chem. Rev.* **2006**, *250*, 3219−3244.

TABLE 1. Protonation Constants (log K_i^H) of [26]phen$_2$N$_4$O$_2$ and Other Related Macrocycles[a]

equilibrium quotient	[26]phen$_2$N$_4$O$_2$[b]	[24]N$_6$O$_2$[c]	[26]*p*bz$_2$N$_4$O$_2$[d]
[HL]/[L][H]	9.62(1)	9.62	9.42
[H$_2$L]/[HL][H]	8.22(2)	8.89	8.74
[H$_3$L]/[H$_2$L][H]	7.31(2)	8.29[c]	7.86
[H$_4$L]/[H$_3$L][H]	5.83(2)	7.62[c]	7.05
[H$_5$L]/[H$_4$L][H]	1.84(2)	3.82[c]	
	1.85(5)[e]		
	2.04(5)[f]		
[H$_6$L]/[H$_5$L][H]	0.89(9)[e]	3.32[c]	
	0.53(9)[f]		
[H$_4$L]/[L][H]^4	30.92(3)	34.42[c]	33.07

[a] T = 298.2 K; I = 0.10 M in KCl. [b] This work; values in parentheses are standard deviations on the last significant figures. [c] I = 0.1 M in KCl.[9] [d] I = 0.1 M in KCl.[10] [e] Value obtained by ^{1}H NMR titration in D_2O and converted to the corresponding value in H_2O using the equation: $pK_D = 0.11 + 1.1 \times pK_H$.[12a] [f] As in footnote *e* but using the equation $pK_H = 0.929 \times pK_{H^*} + 0.42$.[13]

aromatic carboxylates via the establishment of multiple and cooperative electrostatic and hydrogen-bonding interactions. In addition, the molecular recognition of aromatic anions can also involve $\pi-\pi$ stacking interactions between the aromatic moieties of the substrates and those of [26]phen$_2$N$_4$O$_2$.

Compounds incorporating two phen moieties are scarce in the literature, and not all of those have been completely characterized.[5−7] In this work, we present a comprehensive binding solution study that has been carried out with this protonated receptor and with two sets of carboxylic acids that vary in size, charge, rigidity, number of carboxylate groups, and aromaticity degree. One set is composed of aliphatic acids, and the other consists of the aromatic acids that are shown in Chart 1. The synthesis of [26]phen$_2$N$_4$O$_2$ and the crystal structures of the $\{(H_5[26]phen_2N_4O_2)X_n(H_2O)_{5-n}\}X_{n-1}\cdot mH_2O$ supermolecules are also reported, where X = Cl, n = 3, and m = 6 or X = Br, n = 4, and m = 5.5.

Results and Discussion

Synthesis. The macrocycle [26]phen$_2$N$_4$O$_2$ was prepared via a [2 + 2] cycloaddition reaction of 1,10-phenanthroline-2,9-dicarboxaldehyde[8] with 2,2′-oxydiethylamine followed by a reduction with sodium borohydride as described for related compounds.[5] The compound was isolated as bromide and chloride salts in 30 and 20% yields, respectively.

Acid−Base Behavior of [26]phen$_2$N$_4$O$_2$. To obtain information about the binding ability of the protonated forms of [26]phen$_2$N$_4$O$_2$ with anionic species, the protonation constants of [26]phen$_2$N$_4$O$_2$ were determined by potentiometry at 298.2 K in water and in 0.10 M KCl; the results are shown in Table 1 together with those reported for two other structurally related

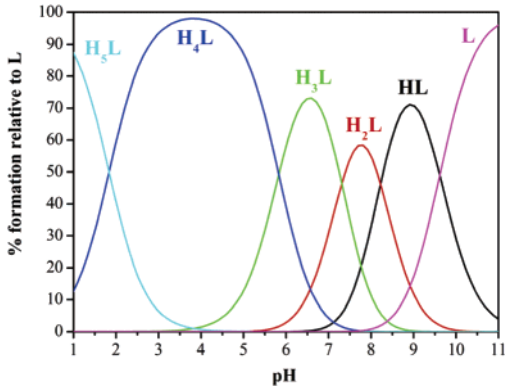

FIGURE 1. Distribution curves diagram of [26]phen$_2$N$_4$O$_2$ using HySS program.[11] $C_L = 2 \times 10^{-3}$ M, where L = [26]phen$_2$N$_4$O$_2$. The charges were omitted for clarity.

2,2′-oxidiethylamine macrocycles, [24]N$_6$O$_2$[9] and [26]*p*bz$_2$N$_4$O$_2$; see Chart 2.[10]

Five protonation constants were found for [26]phen$_2$N$_4$O$_2$, but the lowest value of 1.84 is within the lower limit of the range where it is possible to obtain results by potentiometry. The overall basicity of [26]phen$_2$N$_4$O$_2$ is lower as compared to [24]N$_6$O$_2$ and [26]*p*bz$_2$N$_4$O$_2$ because of the electron withdrawing effect from the phen moiety.

The first four constants correspond to the successive protonation of the secondary nitrogen atoms. The values are those expected for the protonation of amines surrounded by one oxygen atom and one phen unit. The first two values are higher due to (1) statistical factors; (2) long diagonal distance between the amines where the protonation occurs, which decreases the electrostatic effect derived from the formation of the ammonium positive charges; and (3) possible formation of hydrogen bonds N−H···N or N−H···O. The next two protonation constants are obviously lower due to the cumulative positive charges of the macrocycle and the possible disruption of hydrogen bonds. The fifth constant likely occurs on one phenanthroline unit, as is also seen in the related macrocycle R$_2$[26]phen$_2$N$_6$ (with two N-pendent arms, R = 2-(aminoethyl)-2-naphtalen-1-ylmethyl, see Chart 2)[7] and in the X-ray structure; as described below.

The corresponding distribution curve diagram, represented in Figure 1, shows that the tetraprotonated form, H_4L^{4+}, is the main species in solution in the 2−5.5 pH range.[11] The H_5L^{5+} species exists as the main species only at pH values lower than 2.

To confirm the protonation scheme of [26]phen$_2$N$_4$O$_2$ and to determine the lower protonation constants, the ^{1}H NMR titration was performed in D_2O, and the curves are shown in Figure 2. Six resonances were found, which were straightforwardly assigned. The three high field peaks consist of one singlet (H_d) and two triplets (H_e and H_f); the protons of H_f are deshielded by the nearby oxygen atom and are, therefore, assigned to the triplet at lower field. The three phen resonances at low field, which consist of one singlet (H_a) and two doublets (H_b and H_c), are assigned by NOESY experiments at pD 2.5. Cross-peaks were observed between the doublet H_c and the singlet H_d and

(5) Krakowiak, K. E.; Bradshaw, J. S.; Jiang, W.; Dalley, N. K.; Wu, G.; Izatt, R. M. *J. Org. Chem.* **1991**, *56*, 2675−2680.
(6) Keipert, J. S. J.; Knobler, C. B.; Cram, D. J. *Tetrahedron* **1987**, *43*, 4861−4874.
(7) Pina, J.; Melo, J.; Pina, F.; Lodeiro, C.; Lima, J. C.; Parola, A.; Soriano, C.; Clares, M. P.; Albelda, M. T.; Aucejo, R.; García-España, E. *Inorg. Chem.* **2005**, *44*, 7449−7458.
(8) Chandler, C. J.; Deady, L. W.; Reiss, J. A. *J. Heterocycl. Chem.* **1981**, *18*, 599−601.
(9) Shangguan, G.; Martell, A. E.; Zhang, Z.; Reibenspies, J. H. *Inorg. Chim. Acta* **2000**, *299*, 47−58.
(10) Carvalho, S.; Delgado, R.; Drew M. G. B.; Félix, V.; Figueira, M.; Henriques, R. T., unpublished results.
(11) Alderighi, L.; Gans, P.; Ienco, A.; Peters, D.; Sabatini, A.; Vacca, A. *Coord. Chem. Rev.* **1999**, *184*, 311−318.

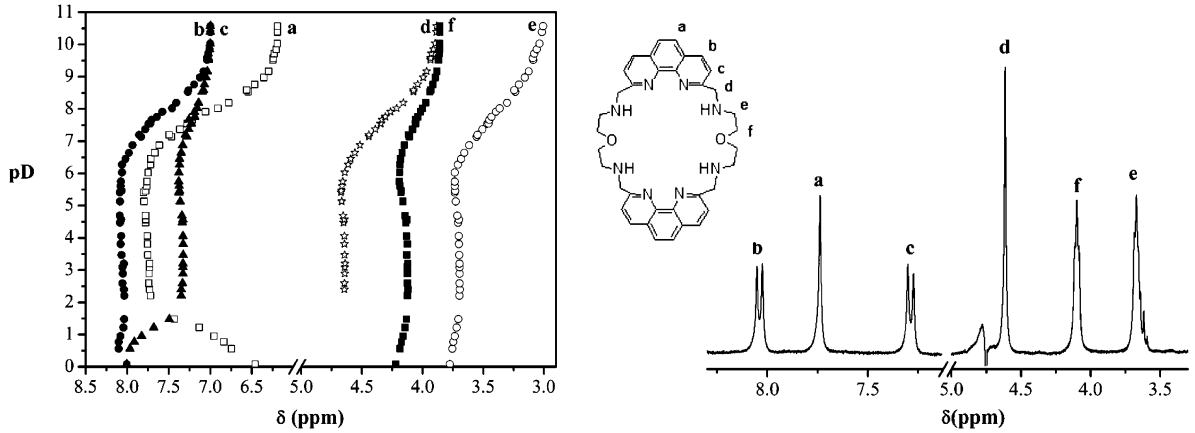

FIGURE 2. ^{1}H NMR titrations curves, pD versus δ (ppm), of [26]phen$_2$N$_4$O$_2$ (left) and one spectrum at pD 3.0 with the structure of the molecule with the labeling scheme adopted (right).

also between the latter resonance and the triplet H_f; H_b has been assigned as the doublet located at lower field and H_e has been assigned as the triplet located upfield. The H_d resonance is included in the water resonance at pD $\leq$ 2 and is impossible to follow. All of the resonances shift to downfield between pD 10 and 5.5, but as expected, H_f and H_c have a lower shift, which can be ascribed to the protonation of the four amine nitrogen atoms. At pD $\leq$ 2 the resonances H_d, H_e, and H_f shift only slightly, whereas resonances H_a and H_c have significant shifts, but H_a shifts in the opposite direction.

The protonation constants as determined from this titration were converted to K_{H_2O} and are included in Table 1. Six protonation constants could be obtained by this technique. The additional constant was determined using the data at very low pD values, which was converted to log K_6 (H_2O).[12,13]

Supramolecular Associations Between {(H$_5$[26]phen$_2$N$_4$O$_2$)}$^{5+}$ and Cl$^-$ and Br$^-$ Anions. The single-crystal structures of the [26]phen$_2$N$_4$O$_2$ as bromide (**2**) and chloride (**1**) salts were determined by X-ray diffraction, and both unequivocally showed that the receptor was pentaprotonated, with the protons bonded to the aliphatic nitrogen donors and to one aromatic nitrogen atom. The content of the two asymmetric units is consistent with the molecular formula $\{(H_5[26]phen_2N_4O_2)X_n(H_2O)_{5-n}\}X_{n-1}\cdot mH_2O$, where X = Cl, n = 3, and m = 6 for **1** and X = Br, n = 4, and m = 5.5 for **2**. The molecular structures of the two supermolecules $\{(H_5[26]phen_2N_4O_2)X_n(H_2O)_{5-n}\}^{(5-n)+}$, presented in Figure 3, show that, in the solid state, the $\{H_5[26]phen_2N_4O_2\}^{5+}$ receptor adopts a horseshoe conformation with enough room to lodge three or four halogen anions. The two phen units are almost parallel and make dihedral angles of 3.1(1) and 1.3(1)° in **1** and **2**, respectively.

The distance between the two aromatic fragments is ca. 6.6 Å in both compounds, which leaves enough space for the selective uptake of aromatic substrates that are intercalated between the two phen units and are stabilized by $\pi-\pi$ stacking interactions, see below. On the other hand, the cavity size given by the average diagonal distance between secondary N−H binding sites is 7.67 Å for **1** and 7.03 Å for **2**, which allows for

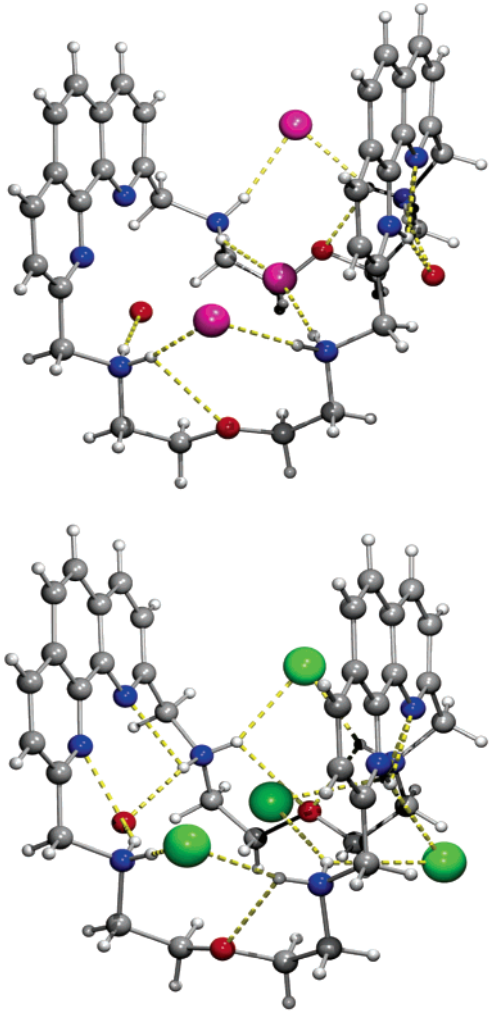

FIGURE 3. Molecular structures of **1** (top) and **2** (bottom). Color scheme: chloride (pink), bromide (green), nitrogen (blue), oxygen (red), carbon (gray) and hydrogen atoms (white).

the molecular recognition of substrates with different sizes and steric requirements via electrostatic and hydrogen-bonding interactions. Indeed, structures **1** and **2** reveal that one halogen anion is clearly encapsulated into the macrocyclic cavity through the formation of two N−H···X hydrogen bonds with the

(12) (a) Delgado, R.; Fraústo da Silva, J. J. R.; Amorim, M. T. S.; Cabral, M. F.; Chaves, S.; Costa, J. *Anal. Chim. Acta* **1991**, *245*, 271−282. (b) Galster, H. *pH Measurement. Fundamentals, Methods, Applications, Instrumentation*; VCH: Weinheim, 1991.

(13) Krężel, A.; Bal, W. *J. Inorg. Biochem.* **2004**, *98*, 161−166.

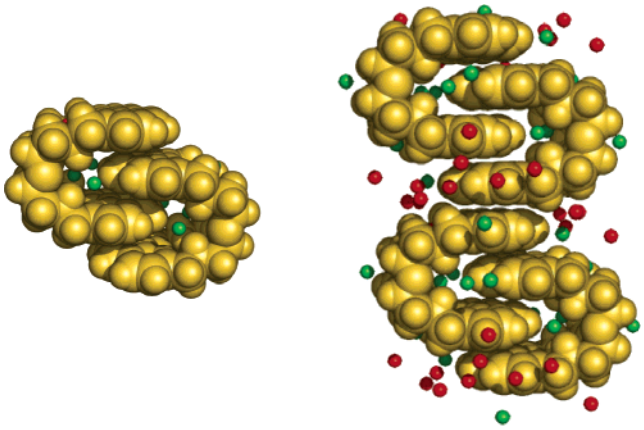

FIGURE 4. Crystal structure of **2**: side view of the two interpenetrated supermolecules composed of two units of **2** (left); 1-D extended aggregate based on $\pi-\pi$ stacking of dimer units (right). Oxygen atoms from water molecules are in red, bromide atoms are in green, and receptors are in yellow.

aliphatic N−H binding sites located at cis and trans relative positions for **1** and **2**, respectively; see Figure 3. The bromide is located 0.432(1) Å away from the N_4 plane, as determined by the aliphatic nitrogen donors, and leads to H···Br distances of 2.49 and 2.81 Å, whereas the chloride is only 0.07(4) Å from that plane, and the H···Cl distances are 2.37 and 2.25 Å. In both supermolecules, the two aliphatic N−H binding sites of the same spacer are connected by two independent halogen bridges with X···H distances ranging from 2.24−2.42 Å for **1** and 2.39−2.50 Å for **2**. The aromatic N−H binding site is also bridged with an N−H aliphatic binding site via N−H···O and N−H···Br bonds that are established with a water molecule in **1** and the fourth bromide counterion in **2**, respectively. The receptor also interacts with a second crystallization water molecule through a single N−H···O hydrogen bond in **1** and two bonds in **2**. Both supermolecules also display several N−H···N and N−H···O intramolecular hydrogen bonds, listed in Table S1 (see Supporting Information). The cooperative effect that is derived from the presence of these multiple hydrogen bonds undoubtedly contributes to the stabilization of the macrocyclic horseshoe topology.

One of the most interesting structural features of the compounds **1** and **2** is revealed by their crystal packing diagrams, which are illustrated in Figure 4 for **2**.

Two $\{(H_5[26]phen_2N_4O_2)X_n(H_2O)_{5-n}\}^{(5-n)+}$ units are self-assembled in a key−lock fashion to form an interpenetrating supermolecule that is stabilized by $\pi-\pi$ interactions between the two aromatic moieties from two receptor units, which adopt an almost parallel arrangement. The corresponding interplanar distances, of ca. 3.3 Å in **1** and **2** (see above), are about half of the distance between the two phen units in the receptor, which shows that it provides a cavity with the appropriate size for the establishment of this type of supramolecular architecture. Additionally, in both compounds, neighboring $\{(H_5[26]phen_2N_4O_2)X_n(H_2O)_{5-n}\}^{(5-n)+}$ supermolecules are packed via $\pi-\pi$ interactions with their phen rings located at interplanar distances of 3.4 Å for **1** and 3.3 Å for **2**, which leads to the formation of one-dimensional (1-D) supramolecular aggregates.

The formation of the supramolecular dimeric entities was confirmed by the ESI-MS^n spectrum (negative ion mode) of **2**, which shows two peaks at *m*/*z* 1798.8 and 1637.1, and is consistent with supramolecular assemblages composed of two receptor units and seven and five bromide anions, respectively. The spectrum shows a set of peaks resulting from the successive loss of bromide anions.

TABLE 2. Overall (log $\beta_{H_hL_1A_a}$)[a] and Stepwise (log $K_{H_hL_1A_a}$) Binding Constants for the Indicated Equilibria[b]

equilibrium process	ox^{2-}	mal^{2-}	suc^{2-}	cit^{3-}	cta^{3-}
$7H^+ + L + A \rightleftarrows H_7LA$					47.20(4)
$6H^+ + L + A \rightleftarrows H_6LA$	40.22(2)	41.45(5)		43.75(2)	43.70(3)
$5H^+ + L + A \rightleftarrows H_5LA$	37.92(2)	38.68(4)	38.37(5)	39.61(3)	39.40(3)
$4H^+ + L + A \rightleftarrows H_4LA$	33.88(3)	33.81(3)	33.76(3)	34.48(2)	34.39(3)
$3H^+ + L + A \rightleftarrows H_3LA$	27.64(3)	27.66(3)	27.88(3)	28.05(3)	28.23(3)
$2H^+ + L + A \rightleftarrows H_2LA$	20.11(2)	20.30(3)	20.40(4)	20.45(5)	
stepwise constants					
$H_5L + HA \rightleftarrows H_6LA$	3.59	3.36			
$H_4L + H_3A \rightleftarrows H_7LA$					2.91
$H_4L + H_2A \rightleftarrows H_6LA$	4.05	2.54		2.69	3.16
$H_4L + HA \rightleftarrows H_5LA$	3.13	2.42	2.15	2.91	3.25
$H_4L + A \rightleftarrows H_4LA$	2.90	2.83	2.78	3.50	3.41
$H_3L + H_2A \rightleftarrows H_5LA$					
$H_3L + HA \rightleftarrows H_4LA$					
$H_3L + A \rightleftarrows H_3LA$	2.49	2.51	2.73	2.90	3.08
$H_2L + A \rightleftarrows H_2LA$	2.27	2.47	2.56	2.62	

[a] Values in parentheses are standard deviations for the last significant figure. [b] L = [26]$phen_2N_4O_2$ and A = anion. I = 0.10 M in KCl at 298.2 K. Charges omitted for clarity.

Binding Studies with Organic Substrates in Water Solution. Potentiometric Measurements. The binding constants of $H_i[26]phen_2N_4O_2^{i+}$ (i = 2−5) with the anions represented in Chart 1 were determined in aqueous solutions at 298.2 K and in 0.10 M KCl using the HYPERQUAD program.[14] The values obtained are collected in Table 2 for aliphatic carboxylate substrates and in Table 3 for aromatic carboxylates. The protonation constants of the anionic substrates contribute significantly to the final stepwise binding constants, and the values from the literature exhibit large discrepancies;[15,16] those values were also determined in the experimental conditions used in this work and are compiled in Table 4, except for Hpyrc, which was taken from ref 16.

Only species with a 1:1 stoichiometry between the receptor (L) and the anions (A) were found for all systems. Several species with different protonation states were found in the pH range 2−8. H_4LA is the main species in the pH range 4−6, whereas at low pH values the H_5LA, H_6LA, and H_7LA species predominate, and at pH > 6, H_3LA and H_2LA also exist. This is illustrated in Figure 5 with the distribution curves diagram for the tph^{2-} as anion.[11]

The receptor and anions participate in several protonation equilibria; some of them overlap in the different pH regions; see Tables 2 and 3. Consequently, it is not straightforward to decide which stepwise equilibria are involved. For example, for tph^{2-} it is an easy task to establish the reactions that involve the fully deprotonated anion (tph^{2-}) with H_2L^{2+}, H_3L^{3+}, and H_4L^{4+} to form H_2LA, H_3LA^+, and H_4LA^{2+}, respectively. However, can equilibrium reactions such as $H_5L^{5+} + tph^{2-} \rightleftarrows H_5Ltph^{3+}$ or $H_4L^{4+} + H_2tph \rightleftarrows H_6Ltph^{4+}$ be associated with log K values of 6.97 and 3.55, respectively? The direct

(14) Gans, P.; Sabatini, A.; Vacca, A. *Talanta* **1996**, *43*, 1739−1753.
(15) Pettit, L. D.; Powell, H. K. J. *IUPAC Stability Constants Database*, version 5; Academic Software: Timble, U.K., 2003.
(16) (a) Donckt, E. V.; Dramaix, R.; Nasielski, J.; Vogels, C. *Trans. Faraday Soc.* **1969**, *65*, 3258−3262. (b) Zelent, B.; Vanderkooi, J. M.; Coleman, R. G.; Gryczynski, I.; Gryczynski, Z. *Biophys. J.* **2006**, *91*, 3864−3871.

TABLE 3. Overall (log $\beta_{H_hL_1A_a}$) and Stepwise (log $K_{H_hL_1A_a}$) Association Constants for the Indicated Equilibria[a]

equilibrium process	bzc$^-$	naphc$^-$	anthc$^-$	pyrc$^-$	ph^{2-}	iph^{2-}	tph^{2-}	btc^{3-}
$7H + L + A \rightleftarrows H_7LA$								45.73(4)
$6H^+ + L + A \rightleftarrows H_6LA$	39.73(4)	40.35(6)	41.20(4)	43.86(5)		41.38(4)	42.60(5)	43.35(5)
$5H^+ + L + A \rightleftarrows H_5LA$	37.68(3)	38.76(4)	38.90(4)	41.81(5)	39.26(1)	39.46(2)	39.79(3)	41.68(2)
$4H^+ + L + A \rightleftarrows H_4LA$	33.70(3)	35.03(4)	34.76(4)	36.61(5)	34.06(2)	36.07(1)	35.72(3)	37.57(1)
$3H^+ + L + A \rightleftarrows H_3LA$	27.46(5)	28.81(4)	28.39(6)	29.91(6)	27.72(3)	28.35(3)	28.91(3)	29.67(1)
$2H^+ + L + A \rightleftarrows H_2LA$		21.13(5)			20.26(4)		21.09(5)	
				stepwise constants				
$H_5L + H_2A \rightleftarrows H_7LA$								4.85
$H_4L + H_3A \rightleftarrows H_7LA$								4.22
$H_5L + HA \rightleftarrows H_6LA$	2.90	4.07	4.68	7.05		4.20		6.03
$H_4L + H_2A \rightleftarrows H_6LA$						2.74	3.55	4.30
$H_4L + HA \rightleftarrows H_5LA$	2.69	4.32	4.22	6.83	3.30	4.12	4.51	6.20
$H_4L + A \rightleftarrows H_4LA$	2.72	4.05	3.78	5.63	3.08	5.09	4.74	6.59
$H_3L + HA \rightleftarrows H_4LA$								
$H_3L + A \rightleftarrows H_3LA$	2.31	3.66	3.24	4.76	2.57	3.20	3.76	4.52
$H_2L + A \rightleftarrows H_2LA$		3.29			2.42		3.25	

[a] L = [26]phen$_2$N$_4$O$_2$ and A = anion. I = 0.10 M in KCl at 298.2 K. Charges omitted for clarity. Values in parentheses are standard deviations for the last significant figure.

TABLE 4. Protonation Constants (log $\beta_{H_hA_a}$) of Anions and the Corresponding Stepwise Constants, log K[a,b]

acid	log β_1^H	log β_2^H [log K_2^H]	log β_3^H [log K_3^H]
H$_2$ox	3.81(1)	5.19(1) [1.37]	
H$_2$mal	5.28(1)	7.94(1) [2.66]	
H$_2$suc	5.25(1)	9.25(1) [4.00]	
H$_3$cit	5.72(1)	10.08(1) [4.36]	13.00(1) [2.92]
H$_3$cta	5.17(1)	9.56(1) [4.39]	13.30(1) [3.74]
Hbzc	4.01(1)		
Hnaphc	3.46(1)		
Hanthc	3.70(9)		
Hpyrc	4.0[c]		
H$_2$ph	4.98(1)	7.82(1) [2.84]	
H$_2$iph	4.36(1)	7.66(1) [3.30]	
H$_2$tph	4.30(1)	8.08(1) [3.78]	
H$_3$btc	4.50(1)	8.07(1) [3.57]	10.54(1) [2.47]

[a] T = 298.2 K; I = 0.10 M in KCl. [b] Values in parentheses are standard deviations in the last significant figures. [c] Because of the very low solubility of Hpyrc in water, we could not obtain accurate values by potentiometric or spectrophotometric measurements; therefore, we took this value from the literature.[16]

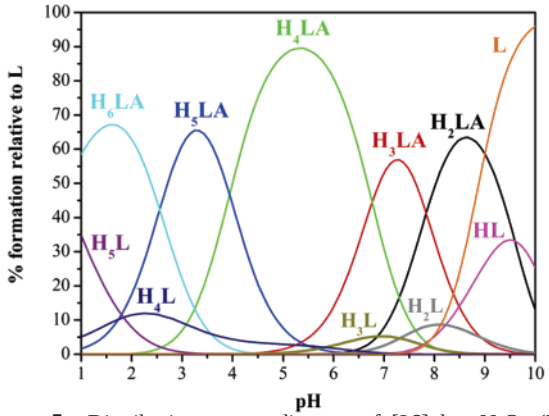

FIGURE 5. Distribution curves diagram of [26]phen$_2$N$_4$O$_2$ (L) in presence of the tph^{2-} anion (A), at $C_L = C_A = 2 \times 10^{-3}$ M. The charges were omitted for clarity.

comparison of stepwise constants of different receptors with an anion can lead to erroneous conclusions and to incorrect attributions of selectivity, as the receptors have different basicities. To overcome these problems, the approach of García-España et al. [17,18] of using effective association constants (K_{eff}) was followed. This value is defined as the quotient of the total amount of supramolecular species formed and the total amounts of the free receptor and substrate at a given pH: $K_{eff} = \sum[LH_nA]/(\sum[H_aA] \times \sum[H_iL])$ (in our case, $n = 2-7$, $a = 0-3$, and $i = 0-5$). These K_{eff} values allow comparisons between different binding supramolecular systems to be carried out under the same experimental conditions.

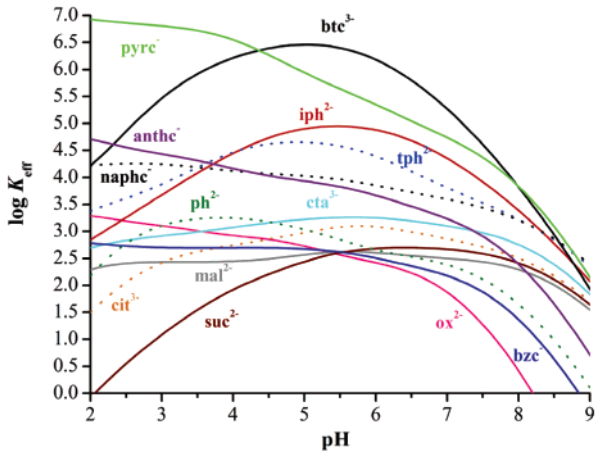

FIGURE 6. Plots of K_{eff} versus pH for the supramolecular associations between [26]phen$_2$N$_4$O$_2$ and the anions presented in Chart 1, $C_L = C_A = 2 \times 10^{-3}$ M.

In Figure 6 is shown the plots of K_{eff} versus pH for the systems between [26]phen$_2$N$_4$O$_2$ and all the studied anions. These plots answer the questions addressed above and are illustrated with the systems containing the tph^{2-} anion and all the other similar ones. Indeed, it is possible to conclude that as the effective constants for the H_i[26]phen$_2$N$_4$O$_2^{i+}$−$H_j$tph^j (i = 2−5 and j = 0−2) system are in the range 2.5−4.5 in log units (in the 2−9 pH range), all of the equilibrium reactions that lead to values significantly outside this range must be discarded.

(17) Albelda, M. T.; Bernardo, M. A.; García-España, E.; Godino-Salido, M. L.; Santiago, V. L.; Melo, M. J.; Pina, F.; Soriano, C. *J. Chem. Soc., Perkin Trans. 2* **1999**, 2545−2549.

(18) Aguilar, J. A.; Celda, B.; Fusi, V.; García-España, E.; Santiago, V. L.; Martínez, M. C.; Ramírez, J. A.; Soriano, C.; Tejero, R. *J. Chem. Soc., Perkin Trans. 2* **2000**, 1323−1328.

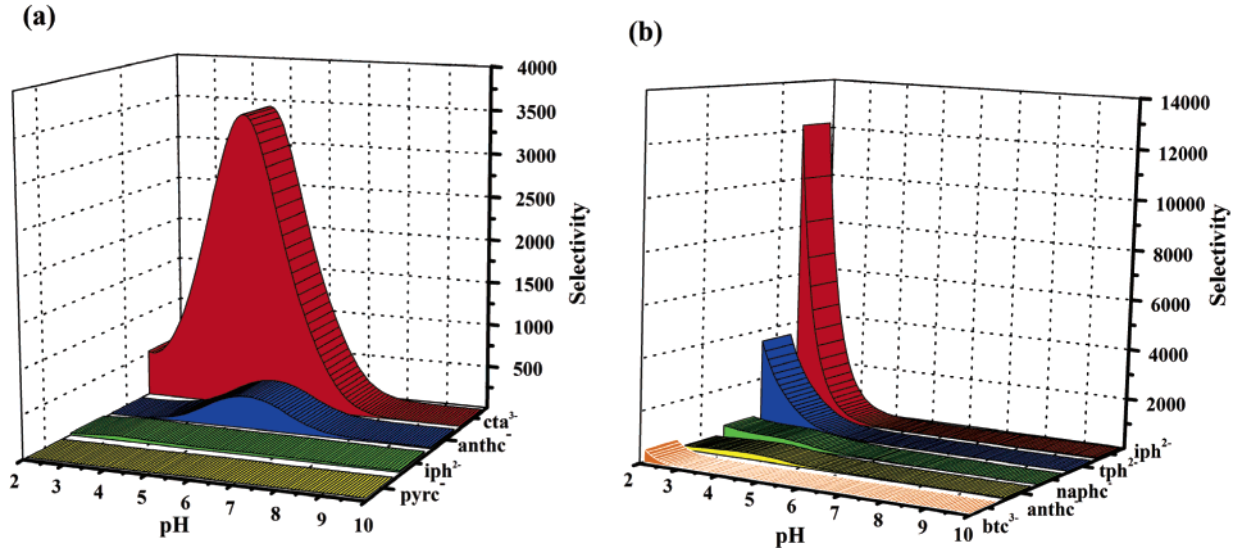

FIGURE 7. Plots of selectivity profile as a function of pH for the interaction of $H_i[26]phen_2N_4O_2^{i+}$ with the following pairs of anions: (a) $btc^{3-}/pyrc^-$, btc^{3-}/iph^{2-}, $btc^{3-}/anthc^-$, and btc^{3-}/cta^{3-}; (b) $pyrc^-/btc^{3-}$, $pyrc^-/anthc^-$, $pyrc^-/naphc^-$, $pyrc^-/tph^{2-}$, and $pyrc^-/iph^{2-}$.

Other important conclusions can also be outlined from Figure 6. The $H_i[26]phen_2N_4O_2^{i+}$ receptor prefers the btc^{3-} anion over a wide pH range (4−8.5), followed by iph^{2-} in a slightly narrow pH region (4.5−8.5) and tph^{2-} (5−7.5). On another hand, $pyrc^-$ exhibits the highest affinity at the lower pH range (<4), followed by $anthc^-$ and $naphc^-$, which is consistent with the increase of the extension of the aromatic rings. However the $pyrc^-$ system has a lower K_{eff} than that of the btc^{3-} in the 4−8.5 pH range, but it is always higher than those of iph^{2-} and tph^{2-}, whereas that for $anthc^-$ crosses the curve of btc^{3-} at very low pH values. The main species in solution are H_6LA^{5+} and H_5LA^{4+} for $pyrc^-$, $anthc^-$, and $naphc^-$, whereas for btc^{3-} they are H_5LA^{2+} and H_4LA^+, and for iph^{2-} and tph^{2-} they are H_5LA^{3+} and H_4LA^{2+}. All of the other anions have effective constants that do not exceed 3.5 log units for the binding with the receptor; among them, cta^{3-} and cit^{3-} have the highest values, due to the stronger electrostatic charge interaction.

The data plotted in Figure 6 also give valuable information about the selective uptake of anions from aqueous solution. Indeed, the quotient of the effective constants for two different anions, at a given pH, allows for the establishment of selectivity ratios. Therefore, the receptor $H_i[26]phen_2N_4O_2^{i+}$ is selective for btc^{3-} when in the presence of all the anions located below tph^{2-} and in the pH range 4−6. However, $pyrc^-$ is the preferred substrate at low pH, as can be seen in Figure 6 or, more appropriately, in diagrams for several anions such as those given in Figure 7. Figure 7a shows that (1) no selectivity is found for the mixture of btc^{3-} and $pyrc^-$ in the presence of our receptor, (2) a very small discrimination exists for the pair $btc^{3-}/anthrc^-$, (3) a selectivity is found for btc^{3-} in the presence of cta^{3-} with the maximum achieved at pH about 5.5. Figure 7b shows that $H_i[26]phen_2N_4O_2^{i+}$ is selective for $pyrc^-$ in the presence of iph^{2-} at pH < 3.5, but it is not selective for $naphc^-$ or btc^{3-}.

Comparisons with other receptors from the literature are also possible. Figure 8, panels a+b show that $H_i[26]phen_2N_4O_2^{i+}$ is the best receptor for the uptake of iph^{2-} and btc^{3-}, respectively,

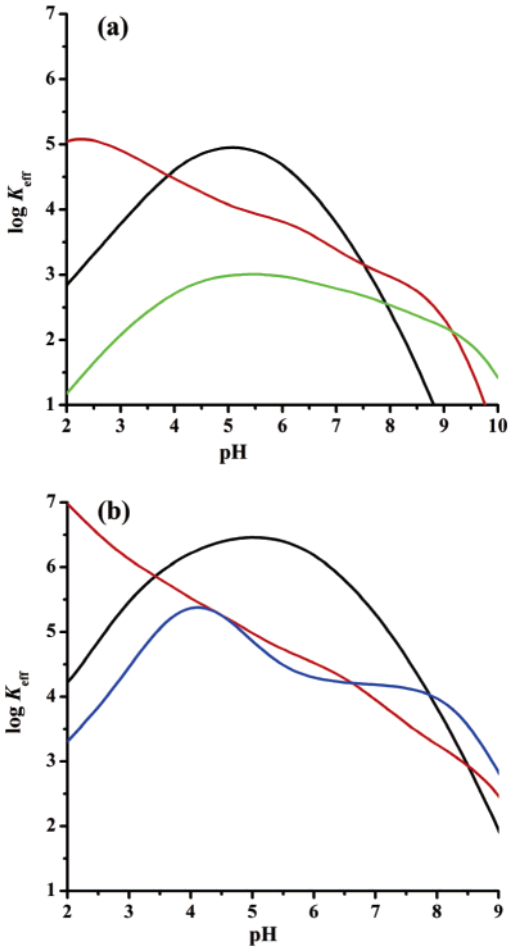

FIGURE 8. Plots of K_{eff} versus pH for the (a) iph^{2-} and (b) btc^{3-} with $H_i[26]phen_2N_4O_2^{i+}$ and three other receptors: $[21]aneN_7$ (red), $[30](chN_2)_3pbz_3$ (blue), $Me_2[30]pbz_2N_6$ (green), and $[26]phen_2N_4O_2$ (black); see Chart 2.

when compared with other recognized good receptors for these anions.[19−21]

^{1}H NMR Spectroscopic Measurements. To obtain further insights into the type of interactions between the substrate

(19) Bencini, A.; Bianchi, A.; Burguete, M. I.; Dapporto, P.; Doménech, A.; García-España, E.; Santiago, V. L.; Paoli, P.; Ramírez, J. A. *J. Chem. Soc., Perkin Trans. 2* **1994**, 569−577.

TABLE 5. Binding Constants (log *K*)[a] of $\{(H_4[26]phen_2N_4O_2)\}^{4+}$ with Selected Anions[b]

anion	log *K*
ox^{2-}	2.59(2)
ph^{2-}	3.23(3)
iph^{2-}	4.77(9)
btc^{3-}	>5.0
cta^{3-}	3.08(1)

[a] Values in parentheses are standard deviations in the last significant figures given directly by the program.[22] [b] Determined in D_2O at 298.2 K.

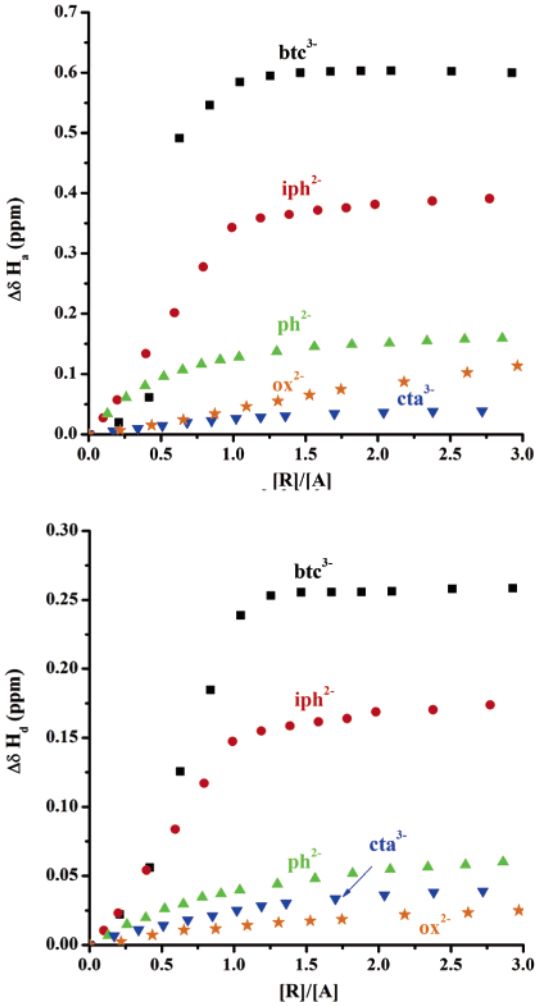

FIGURE 9. Δδ ^{1}H NMR shift of H_a (top) and H_d (bottom) of $\{H_4[26]phen_2N_4O_2\}^{4+}$ as a function of the number of equivalents of anionic substrate added, in D_2O. The symbols for anions are btc^{3-} (■), iph^{2-} (red ●), ph^{2-} (green ▲), cta^{3-} (blue ▼) and ox^{2-} (yellow ★).

$H_4[26]phen_2N_4O_2^{4+}$ and selected anions (btc^{3-}, iph^{2-}, ph^{2-}, cta^{3-}, and ox^{2-}) and about the identification of the possible location of the encapsulated substrate into the receptor, ^{1}H NMR spectroscopic titrations were performed in D_2O at pD 5. The high accuracy of the titrations allowed for the determination of the binding constants using the HypNMR[22] program, and the results are collected in Table 5.

For all of the studied substrates, the plot of the variation of the chemical shift versus [R]/[A] (R for receptor and A for substrate) shows a profile that is consistent with the formation of 1:1 stoichiometric supramolecular association between the receptor and the substrates, as shown in Figure 9. This was confirmed by the corresponding Job's plot.[23] The values are in good agreement to those determined by potentiometry, when considering that the ^{1}H NMR titration curves were obtained in a different medium, the ionic strength was not controlled, and no buffer was used to maintain the pH. In spite of this, the pD of the solution has a variation of less than 0.5 pH units.

Every resonance of the free receptor shifts highfield, except for that of H_c. The larger shift is observed for H_a, followed by H_d for the aromatic substrates, whereas for cta^{3-} and ox^{2-} both resonances have similar shifts. Resonances for H_e and H_f exhibit much smaller shifts for the aromatic substrates, whereas they are smaller but of the same order of the other two resonances for cta^{3-} and ox^{2-}. These features suggest that all of the ammonium donor atoms as well as the aromatic regions of the receptor are involved in the molecular recognition of the aromatic substrates, whereas only electrostatic and hydrogen bonds of the type $^+N-H\cdots{}^-O$ are involved for cta^{3-}.

NOESY experiments were performed on the supramolecular entities that were formed with btc^{3-} and iph^{2-} and the $(H_4[26]phen_2N_4O_2)^{4+}$ at pD 5 in D_2O at room temperature to locate the substrate in the organized structure of the receptor. With btc^{3-}, cross-peaks were observed between the singlet resonance of the substrate with the three aromatic signals (strong intensity) and also with H_d, H_e, and H_f (lower intensity) of the receptor, see Supporting Information. However, in the case of iph^{2-}, cross-peaks were observed only between the two highfield proton resonances of the substrate and H_a and H_b of the receptor. These features strongly suggest that the btc^{3-} is encapsulated by the receptor via $\pi-\pi$ stacking interactions and $^+N-H\cdots{}^-O$ hydrogen bonds, whereas iph^{2-} mainly interacts with the aromatic part of the receptor.

Molecular Modeling Studies. The molecular modeling of the binding recognition process between the protonated receptor and the anions is not straightforward because, in aqueous solution, as demonstrated above, several H_iLA^{n+} species can coexist, as derived from the competitive equilibriums. Here we describe the preliminary results of molecular mechanics (MM) and molecular dynamics (MD) simulations studies carried out with $(H_5[26]phen_2N_4O_2)^{5+}$ and seven completely deprotonated aromatic anions (bzc^-, iph^{2-}, ph^{2-}, $anthc^-$, $naphc^-$, $pyrc^-$, and btc^{3-}) by using the general amber force field[24] (GAFF) within the Amber-8 software package.[25] The main purpose of this modeling investigation was to evaluate the role of the $N-H\cdots O$ hydrogen bonds pattern and the possible $\pi-\pi$ interactions between the aromatic ring of the substrate and two phen units of receptor present in the formation of H_5LA^{n+} species. Therefore, the anions were selected by taking into

(20) Carvalho, S.; Delgado, R.; Fonseca, N.; Félix, V. *New J. Chem.* **2006**, *30*, 247−257.
(21) Hodacová, J.; Chadim, M.; Závada, J.; Aguilar, J.; García-España, E.; Santiago, V. L.; Miravet, J. F. *J. Org. Chem.* **2005**, *70*, 2042−2047.
(22) Frassineti, C.; Ghelli, S.; Gans, P.; Sabatini, A.; Moruzzi, M. S.; Vacca, A. *Anal. Biochem.* **1995**, *231*, 374−382.
(23) (a) Sebo, L.; Diederich, F.; Gramlich, V. *Helv. Chim. Acta* **2000**, *83*, 93−113. (b) Hirose, K. *J. Inclusion Phenom. Macrocyclic Chem.* **2001**, *39*, 193−209.
(24) GAFF force field, Wang, J.; Wolf, R. M.; Caldwell, J. W.; Kollmann, P. A.; Case, D. A. *J. Comput. Chem.* **2004**, *25*, 1157−1174.
(25) *Amber*, version 8; Case, D. A.; Darden, T. A.; Cheatham, T. E., III; Simmerling, C. L.; Wang, J.; Duke, R. E.; Luo, R.; Merez, K. M.; Wang, B.; Pearlman, D. A.; Crowley, M.; Brozell, S.; Tsui, V.; Gohlke, H.; Mongan, J.; Hornak, V.; Cui, G.; Beroza, P.; Schafmeister, C.; Caldwell, J. W.; Ross, W. S.; Kollman, P. A. University of California: San Francisco, 2004.

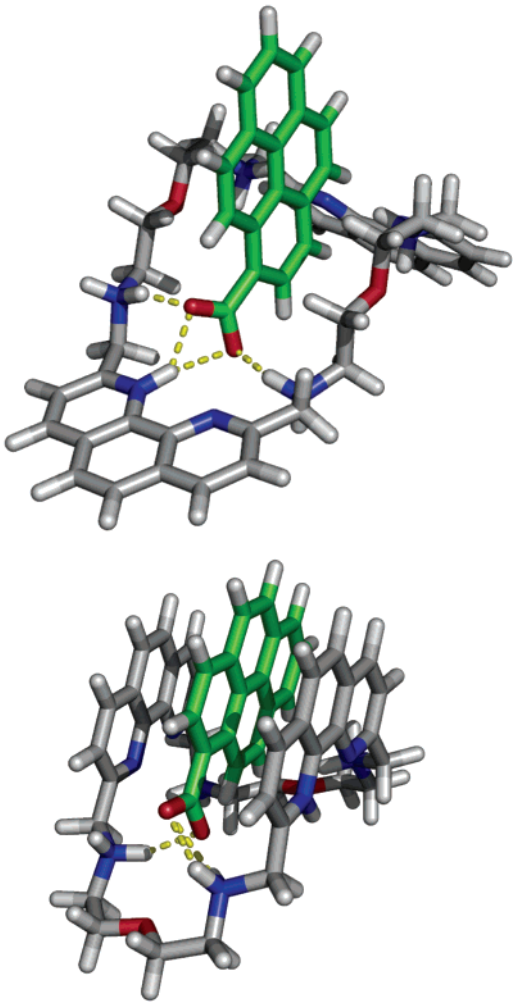

FIGURE 10. Lowest energy structures found in the conformational analysis of $\{(H_5[26]phen_2N_4O_2)(pyrc)\}^{4+}$: arrangements A (top) and B (bottom) with the carbon atoms of the receptor and anion shown in green and gray respectively.

account the extension of its aromatic systems and the number and the relative position of carboxylate groups.

The docking between the receptor and the anion was carried out in the gas phase via MD quenching runs, as described below in the experimental section. The lowest energy geometric arrangement found for all mono-carboxylate anions shows that the macrocycle with two phen units adopts an almost planar spatial disposition that is between a slightly twisted and slightly bent arrangement. The anion was strongly bound to the N−H aliphatic binding sites of the receptor via N−H···O hydrogen bonds (arrangement A). By contrast, for substrates having two (iph^{2-} and ph^{2-}) or three carboxylate groups (btc^{3-}), the lowest energy structure displayed the receptor in the horseshoe shape conformation, which is similar to that found in the crystal structures, and the anion is inserted between two aromatic phen units with oxygen atoms from carboxylate groups forming hydrogen-bonding interactions with secondary N−H binding sites (arrangement B). The two geometric arrangements for $\{H_5[26]phen_2N_4O_2)(pyrc)\}^{4+}$ are shown in Figure 10. The difference in energy [E(B) − E(A)] between the two geometric arrangements decreases with the enlargement of the aromatic system of the substrate, 17.4 kcal·mol^{-1} for bzc^-, 13.5 kcal·mol^{-1} for $naphc^-$, 8.1 kcal·mol^{-1} for $anthc^-$, and only 1.0 kcal·mol^{-1} for $pyrc^-$, which shows that arrangement B is not favored. However for the ph^{2-}, iph^{2-}, and btc^{3-} anions the difference is −13.0, −14.0, and −33.3 kcal·mol^{-1}, respectively, which indicates that arrangement B is now the preferred one. Subsequent MD simulations were carried out in solution at 300 K for 5 ns using an explicit model of water for the supramolecular associations with $naphc^-$, iph^{2-}, and $pyrc^-$ in both geometries. The MM energy of each supramolecular entity was calculated by postprocessing the trajectories files using the MM-PBSA method as described below.[26] The energetic difference between the arrangements B and A is −132.2 kcal·mol^{-1} for iph^{2-} and −18.5 kcal·mol^{-1} for $naphc^-$, which indicates that the first one is also favored in water solution and is in the trend line with docking results.

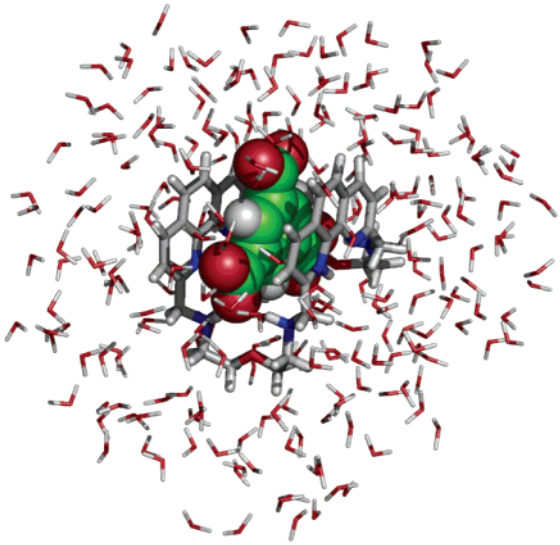

FIGURE 11. Snapshot taken at 3 ns of MD simulation that illustrates the molecular recognition between the receptor and the btc^{3-} substrate, which are represented as stick and space filling models, respectively. For clarity, only the 250 water solvent molecules and the supermolecule are shown. The two Cl^- counterions are omitted.

By contrast, arrangement B is now undoubtedly preferred by 82.6 kcal·mol^{-1} for $pyrc^-$. The analysis of the hydrogen bonds over trajectory files for all systems shows that, in the solvent water solution as in the gas phase, the molecular recognition process occurs through the establishment of multiple, cooperative N−H···O hydrogen-bonding interactions between the receptor and the substrate. Throughout the duration of the simulation for the iph^{2-} and btc^{3-} anions, hydrogen bonds between two carboxylates groups and several binding N−H binding sites from two oxadiaza spacers were observed. Furthermore, in these two anions with two or three carboxylate groups or those containing extended aromatic systems, such as $pyrc^-$, the hydrogen bond pattern is complemented by $\pi-\pi$ stacking bonding contacts, and the anion is encapsulated into the macrocyclic cavity between two phen aromatic units, which creates a structure that is consistent with the experimental results. The binding interaction between the aromatic substrates and the receptor in solution is illustrated in Figure 11 for the btc^{3-} anion.

Conclusions. The design of a novel receptor with selective binding affinity for aromatic carboxylate substrates is reported.

(26) Kollman, P. A.; Massova, I.; Kuhn, B.; Huo, S.; Chong, L.; Lee, M.; Lee, T.; Duan, Y.; Wang, W.; Donni, O.; Cieplak, P.; Srinivasan, J.; Case, D. A.; Cheatham, T. E., III *Acc. Chem. Res.* **2000**, *33*, 889−897.

The values of the binding constants revealed that the affinity of the $H_i[26]phen_2N_4O_2^{i+}$ receptor increases with the number of coupled aromatic units and with the number of carboxylate groups (or net charge) of the substrate; consequently, the largest values of the association constants were found for $pyrc^-$ and btc^{3-} anions, respectively. Therefore, the $H_i[26]phen_2N_4O_2^{i+}$ receptor can be used for the uptake of btc^{3-} and $pyrc^-$ from a solution containing other carboxylate substrates at pH values of ca. 5.5 and 3.0, respectively. Our studies also show that the relative positions of the two carboxylate groups in iph^{2-}, ph^{2-}, and tph^{2-} are responsible for the different binding affinities.

Experimental and molecular modeling studies are consistent in showing that the recognition process between the receptor and the substrates is based on multiple and cooperative $^+N-H\cdots{}^-O$ hydrogen bonds and electrostatic and/or $\pi-\pi$ stacking binding interactions.

The crystal structures of $H_5[26]phen_2N_4O_2^{5+}$ with chloride or bromide and the corresponding mass spectra studies showed the formation of supramolecular assemblages composed of two receptor units, which prompts us to think that the insertion mechanism of the substrate into the receptor cage involves a first step of unlocking the interpenetrated supermolecule composed of two $\{(H_5[26]phen_2N_4O_2)X_n(H_2O)_{5-n}\}^{(5-n)+}$ units. The study of this particular feature and of the binding affinity determination for other related receptors containing two phen units toward a wide range of anionic substrates, using a combination of theoretical and experimental methods, is in progress in our laboratories.

Experimental

Reagents. 1,10-Phenanthroline-2,9-dicarboxaldehyde was prepared by the reaction of 1,10-phenanthroline-2,9-dimethyl with selenium dioxide.[8] All chemicals were of reagent grade and were used as supplied without further purification. The references used for the ^1H and ^{13}C NMR measurements in D_2O were 3-(trimethylsilyl)-propanoic acid-d_4-sodium salt and 1,4-dioxane, respectively.

Synthesis of the Macrocycle [26]phen$_2$N$_4$O$_2$. 1,10-Phenanthroline-2,9-dicarboxaldehyde (50.0 mg, 0.22 mmol) was dissolved in 80 mL of hot methanol and then cooled to r.t. This solution was slowly dropped into a methanol solution (40 mL) containing 2,2′-oxidiethylamine (21.0 mg, 0.22 mmol) over 15−20 min. The resulting mixture was stirred for 16 h. The solid product was filtered off and was then dissolved in ethanol. Sodium borohydride (1.0 g, 26 mmol) was then added in small portions at r.t., and the mixture was stirred for 12 h. The solvent was removed under reduced pressure. The resulting residue was treated with water and was repeatedly extracted with chloroform (6 × 25 mL). The organic phases were combined, completely evaporated under vacuum, and dissolved in ethanol. The pure compound was precipitated from hydrobromic or hydrochloric acid solutions as a white powder that was easy to filter off upon 12 h at low temperature.

Hydrochloric Compound, 1. Yield 20%, mp 203−204 °C. ^1H NMR (300 MHz, D_2O, δ/ppm) 3.65 (8 H, t, NCH_2CH_2O), 4.06 (8 H, t, NCH_2CH_2O), 4.59 (8 H, s, $phenCH_2N$), 7.28 (4 H, d, phen), 7.72 (4 H, s, phen), 8.03 (4 H, d, phen). ^{13}C NMR (300 MHz, D_2O, δ/ppm): δ 49.5 (NCH_2CH_2O), 53.3 (NCH_2CH_2O), 67.7 ($phenCH_2N$), 125, 129, 130.6, 141.1, 144.9, 153.2 (phen). Anal. Calcd for $C_{36}H_{51}N_8O_5Cl_5$: C, 50.68; H, 6.03; N, 13.13%. Found: C, 50.60; H, 6.39; N, 12.66%.

Hydrobromic Compound, 2. Yield 30%, mp 223−224 °C. ^1H NMR (300 MHz, D_2O, δ/ppm) 3.70 (8 H, t, NCH_2CH_2O), 4.13 (8 H, t, NCH_2CH_2O), 4.65 (8 H, s, $phenCH_2N$), 7.32 (4 H, d, phen), 7.80 (4 H, s, phen), 8.08 (4 H, d, phen). ^{13}C NMR (300 MHz, D_2O, δ/ppm): 47.5, 53.9, 68.4, 120.0, 123.6, 125.4, 134.0, 144.8, 158.3. Anal. Calcd. for $C_{36}H_{45}N_8O_2Br_5$: C, 42.34; H, 4.44; N, 10.97%. Found: C, 42.16; H, 4.32; N, 10.48%. ESI-MS, m/z: 1798.8 [2M + 7Br − 2H]$^-$, 1637.1 [2M + 5Br − 6H]$^-$, 1018.6 [M + 5Br − H]$^-$, 938.6 [M + 4Br − 2H]$^-$, 858.9 [M + 3Br − 3H]$^-$, 777.0 [M + 2Br − 4H]$^-$.

Compounds **1** and **2** were dissolved in a small amount of water/methanol (4:1 v/v) solution (1 mL) and left at r.t. Crystals suitable for X-ray diffraction structure determinations were obtained by slow evaporation of the solvent over a week.

Preparation of the Substrates. To a stirred solution of the carboxylic acid (10.0 mmol) in water (20 mL), 1.0 to 3.0 equiv (for the mono-, di-, and tricarboxylic acids, respectively) of a solution of potassium hydroxide (1.0 M) in water was added. The solvent was then evaporated, and the salts were recrystallized from acetone and dried under vacuum.

Potentiometric Measurements. Reagents and Solutions. The aqueous solutions of the anions were standardized with a standard HCl solution. The aliphatic acids were directly standardized with a KOH solution. Carbonate-free solutions of KOH were freshly prepared, maintained in a closed bottle, and discarded when the percentage of carbonate was about 0.5% of the total amount of base (tested by Gran's method).[27]

Equipment and Working Conditions. The equipment used was described previously.[20] The temperature was kept at 298.2 ± 0.1 K; atmospheric CO_2 was excluded from the cell during the titration by passing purified argon across the top of the solution in the reaction cell. The ionic strength of the solutions was kept at 0.10 ± 0.01 M KCl.

Measurements. The $[H^+]$ of the solutions was determined by the measurement of the electromotive force of the cell, $E = E'^\circ + Q \log[H^+] + E_j$. The terms E'°, Q, E_j, and $K_w = ([H^+][OH])$ were obtained as described previously.[20] The term pH is defined as $-\log[H^+]$. The value of K_w was found to be equal to $10^{-13.80}$ M^2. The measurements were carried out using 20.00 mL of $a \sim 1.7 \times 10^{-3}$ M $\{(H_5[26]phen_2N_4O_2)Cl_3\}^{2+}$ solution, and the substrate concentration was varied from 2×10^{-3} to 5×10^{-3} M. At least three titrations were performed in the pH range of 2−10 at 1:1 and 1:2 C_L/C_A ratios (ca. 100 experimental points).

Calculation of Equilibrium Constants. The protonation constants of the receptor and of the substrates, β_i^H, were determined from the experimental data using the Hyperquad program.[14] All of these constants were taken as fixed values in order to obtain the equilibrium constants of the associated species from the experimental data that correspond to titrations of different R:A ratios. The different titration curves of the same system were treated first as a single set; finally, all of the data were merged together and were treated simultaneously to give the final model of binding constants. Moreover, several measurements were made both in formation and in dissociation (from acid to alkaline pH and vice−versa) to check the reversibility of the reactions.

The initial computations were obtained in the form of overall stability constants, β_{H_hLA} values, $\beta_{H_hLA} = [H_hLA]/[H]^h[L][A]$ and stepwise binding constants K_{H_hLA} were obtained by $[H_hLA]/[H_hL][A]$. The errors quoted are the standard deviations of the overall stability constants given directly by the program for the input data, which includes all of the experimental points of all titration curves. The species considered in a particular model were those that could be justified by the principles of supramolecular chemistry.

^{1}H NMR Spectroscopic Titrations. Titration of [26]phen$_2$N$_4$O$_2$. Solutions of $[26]phen_2N_4O_2$ (0.01 M) in D_2O were titrated using DCl (0.1 M in D_2O) or CO_2-free KOD that was freshly prepared (0.10 M), and the $pH^* = -\log[H^*]$ was measured directly in the NMR tube with an instrument fitted with a combined microelectrode. The pH meter was previously calibrated with aqueous buffered solutions at pH 4.00 and 7.20. The final pD was calculated from $pD = pH^* + (0.40 \pm 0.02)$.[12b]

(27) (a) Gran, G. *Analyst (London)* **1952**, *77*, 661−671. (b) Rossotti, F. J.; Rossotti, H. J. *J. Chem. Educ.* **1965**, *42*, 375−378.

The 2D-NOESY experiments were performed by collecting 1024 (t_2) × 512 (t_1) data points using a standard pulse program. A 5.0 μs pulse width, which corresponds to a 90° flip angle, and mixing times of 150 and 500 ms for the receptor (pD = 2.87) and the supramolecular entities (pD = 5.16 for iph^{2-} and 5.70 for btc^{3-}), respectively, were used. The best cross-peak signals were observed for a 1:2 substrate/receptor stoichiometry.

Determination of the Association Constants. **Reagents and Solutions.** Solutions of $(H_4[26]phen_2N_4O_2)^{4+}$ (2.0×10^{-3} M) were prepared by dissolution of the macrocycle in 0.5 cm^{-3} of D_2O, and the pD was adjusted to 5.0. The anion solutions were prepared at $(1.2-2.2) \times 10^{-2}$ M by dissolution of the potassium salts in 0.5 mL of D_2O.

Using a syringe of 25 μL, 0.01 mL portions of the K^+ salt of each carboxylate, which were dissolved in D_2O at 298.2 K, were added to the solution of $(H_4[26]phen_2N_4O_2)^{4+}$ in D_2O. About 15 additions were necessary for each titration, until no further change in the chemical shift was observed, and each solution was left for 15−20 min to stabilize. An effort to maintain a constant ionic strength to avoid the competition of other anions was not made, but care was taken to avoid CO_2 absorption from the atmosphere.

Changes in the chemical shift of each proton were recorded, and the association constants of the various species formed in solution were determined from the experimental data using HypNMR,[22] which requires as input the concentration of each component and the observed chemical shift. Initial calculations provided the overall stability constants, $\beta_{R_rA_a}$ values, of $\beta_{R_rA_a} = [R_rA_a]/[R]^r[A]^a$, where $R = (H_4[26]phen_2N_4O_2)^{4+}$. Only species with a 1:1 stoichiometry were found in all cases. The quoted errors are the standard deviations of the overall stability constants directly given by the program from the input data, which include the experimental points for all resonances of the titration curves. The standard deviations of the stepwise constants, shown in Table 5, were determined by the normal propagation rules.

Job's Plots. Stock solution for the host (concentrations from 2.00 to 3.00 mM) and for the potassium salts of substrates (in the same concentrations) were prepared in D_2O. Ten NMR tubes were filled with 500 μL solutions of the host and guest in the following volume ratios: 50:450, 100:400, 150:350, 200:300, 250:250, 300:200, 350:150, 400:100, 450:50, 500:0. The chemical shift change of the H_b resonance for each solution is measured, and the product between the increment in chemical shift and receptor concentration versus the molar fraction of the receptor was plotted. A curve is generated where the maximum point indicates the stoichiometry of the complex by use of the equation, $[C] = [R]_0 \times (\delta_{obs} - \delta_R)/(\delta_{max} - \delta_R)$, where $[R]_0$ is the total receptor concentration, δ_{obs} is the observed chemical shift, δ_R is the chemical shift of the free receptor, and δ_{max} is the chemical shift of the complex. Because $(\delta_{max} - \delta_R)$ is a constant, the concentration of the complex is proportional to $\Delta\delta \times [R]_0$ [where $\Delta\delta = (\delta_{obs} - \delta_R)$]. Job's plots of iph^{2-} and cta^{3-} were performed, and these curves exhibit a maximum at $X = 0.5$, which indicates a 1:1 complexation.[23]

X-ray Structure Determination of Compounds 1 and 2. The pertinent crystallographic data for compounds **1** and **2** are shown in Table S2 (see Supporting Information). X-ray data were collected at room temperature on an image plate system using graphite monochromatised Mo−Kα radiation ($\lambda = 0.71073$ Å) at Reading University. The crystals were positioned at 70 mm from the image plate; 95 frames were taken at 2° intervals using an appropriate counting time. Data analysis was performed with the XDS program.[28] Intensities of both compounds were corrected for absorption effects empirically by using the DIFABS program.[29]

Both structures were solved by direct methods and by subsequent difference Fourier syntheses and were refined by full matrix least-squares on F^2 using the SHELX-97 suite.[30] Anisotropic thermal parameters were used for all non-hydrogen atoms. Hydrogen atoms bonded to carbon and nitrogen atoms were placed at calculated positions with $U_{iso} = 1.2U_{eq}$ of the parent atom, except for the N−H aromatic atoms, whose positions were retrieved from final difference Fourier maps and refined with individual isotropic thermal parameters. The atomic positions of water hydrogen atoms were not discernible from the last difference Fourier maps, and they were not introduced in the refinement. The residual electronic density, ranging from 0.496 to −0.371 e·Å^{-3} for **1** and 1.234 to −0.688 e·Å^{-3} for **2**, was within the expected values. Molecular diagrams were drawn with Platon[31] and PyMOL.[32]

Molecular Modeling Simulations. MM calculations and MD simulations were carried out using the Amber 8 suite of programs,[25] with parameters for $H_5[26]phen_2N_4O_2^{5+}$ and anions taken from the GAFF designed for organic molecules.[24] The structure of the pentaprotonated receptor was taken from the crystal structure of **1.** The atomic point charges were calculated for the receptor and for anions bzc^-, ph^{2-}, iph^{2-}, btc^{3-}, $naphc^-$, $pyrc^-$ and tph^{2-} at the 6-31G(d) level using the RESP methodology[33] with Gaussian03.[34] The starting models for theoretical binding studies were generated from the crystal structure of the protonated receptor **1**. One molecule of the anion was positioned above the macrocyclic cavity, and the model complex with a stoichiometry of 1:1 was subsequently energy-minimized by MM. The minimized structures were then subjected to a MD quenching run at 2000 K using a time step of 1 fs, and 20 000 gas phase conformations were generated at 0.1 ps intervals. All of them were subsequently minimized by MM using a in-house script.

Further MD simulations in water were performed with both lowest energy geometric arrangements (A and B) found for the complexes between $(H_5[26]phen_2N_4O_2)^{5+}$ and $naphc^-$, iph^{2-}, and $pyrc^-$ anions. Only a unique single geometry was used in the MD simulations for the supramolecular associations with btc^{3-} and bzc^- anions, A and B, respectively. Single solute molecules were solvated using a TIP3P water model[35] with the number of solvent molecules ranging from 1893 to 2008. The electrostatic neutrality of each system was achieved with the replacement of four or five water molecules by an equivalent number of Cl^- anions. The charge of each Cl^- counterion was set to −1 and the van der Waals parameters were taken from ref 36. All MD simulations started with equilibration of the system under periodic boundary conditions using a multistage protocol that was composed of two successive

(28) Kabsch, W. *J. Appl. Crystallogr.* **1988**, *21*, 916−924.
(29) *DIFABS*, Walker, N.; Stuart, D. *Acta Crystallogr.* **1983**, *A39*, 158−166.
(30) *SHELX-97*, Sheldrick, G. M. University of Göttingen: Germany, 1997.
(31) *PLATON: a Multipurpose Crystallographic Tool*, Spek, L., Utrecht University: Utrecht, The Netherlands, 1999.
(32) Delano, W. L. *The Pymol Molecular Graphics System on World Wide Web*, http://www.pymol.org, 2002.
(33) Bayly, C. I.; Cieplak, P.; Cornell, W. D.; Kollman, P. A. *J. Chem. Phys.* **1993**, *97*, 10269−10280.
(34) *Gaussian 03*, Revision C.02; Frisch, M. J.; Trucks, G. W.; Schlegel, H. B.; Scuseria, G. E.; Robb, M. A.; Cheeseman, J. R.; Montgomery, Jr., J. A.; Vreven, T.; Kudin, K. N.; Burant, J. C.; Millam, J. M.; Iyengar, S. S.; Tomasi, J.; Barone, V.; Mennucci, B.; Cossi, M.; Scalmani, G.; Rega, N.; Petersson, G. A.; Nakatsuji, H.; Hada, M.; Ehara, M.; Toyota, K.; Fukuda, R.; Hasegawa, J.; Ishida, M.; Nakajima, T.; Honda, Y.; Kitao, O.; Nakai, H.; Klene, M.; Li, X.; Knox, J. E.; Hratchian, H. P.; Cross, J. B.; Bakken, V.; Adamo, C.; Jaramillo, J.; Gomperts, R.; Stratmann, R. E.; Yazyev, O.; Austin, A. J.; Cammi, R.; Pomelli, C.; Ochterski, J. W.; Ayala, P. Y.; Morokuma, K.; Voth, G. A.; Salvador, P.; Dannenberg, J. J.; Zakrzewski, V. G.; Dapprich, S.; Daniels, A. D.; Strain, M. C.; Farkas, O.; Malick, D. K.; Rabuck, A. D.; Raghavachari, K.; Foresman, J. B.; Ortiz, J. V.; Cui, Q.; Baboul, A. G.; Clifford, S.; Cioslowski, J.; Stefanov, B. B.; Liu, G.; Liashenko, A.; Piskorz, P.; Komaromi, I.; Martin, R. L.; Fox, D. J.; Keith, T.; Al-Laham, M. A.; Peng, C. Y.; Nanayakkara, A.; Challacombe, M.; Gill, P. M. W.; Johnson, B.; Chen, W.; Wong, M. W.; Gonzalez, C.; Pople, J. A.; Gaussian, Inc.: Wallingford CT, 2004.
(35) Jorgensen, W. L.; Chandrasekhar, J.; Madura, J. D.; Impey, R. W.; Klein, M. L. *J. Chem. Phys.* **1983**, *79*, 926−935.
(36) Rao, B. G.; Singh, U. C. *J. Am. Chem. Soc.* **1999**, *112*, 3803−3811.

MM minimizations, to eliminate undesired short potential contacts. Next, an MD−NVT simulation was run to bring the temperature to 300 K; an MD−NPT simulation was then run to adjust the density. During the last period of this simulation, typically 50 ps, the density of the periodic cubic box was within the expected value for the experimental density of the liquid water at room temperature, and the final sizes of all equilibrated boxes were in the range between 38.8 and 39.6 Å. Finally, an MD data collection run was produced at 300 K and 1 atm for 5 ns using an NPT ensemble. All bonds involving hydrogen atoms were constrained using SHAKE,[37] which allowed the use of a time step of 2 fs. The particle mesh Ewald method was used to describe the long-range electrostatic interactions, and the nonbonded van der Waals interactions were subjected to a 12 Å cutoff.

The MM energies for the supramolecular associations in water were calculated by postprocessing the trajectory files of independent simulations that were carried out in both geometric arrangements, A and B, with the MM-Poisson−Boltzmann/surface area (MM-PBSA) method.[26] The average MM energy was calculated using 5000 independent binding scenarios without water molecules and chloride counterions. They were extracted with a frequency of 5 frames from trajectory files containing 25 000 frames saved every 0.2 ps during each MD data collection run. They were subsequently used in the calculation of the average MM energies.

(37) Ryckaert, J. P.; Cicotti, G.; Berendsen, H. J. C. *J. Comput. Phys*. **1977**, *23*, 327−341.

Acknowledgment. Authors acknowledge Helena Matias for technical assistance on 2D-NOESY experiments, and EPSRC and the University of Reading for funds for the Image Plate used. C. C. thanks ITQB for access to the potentiometric and NMR facilities, INETI for the ESI-MS^n data, and FCT for the Ph.D. grant (SFRH/BD/19266/2004). This work has been partially supported by FCT and POCI, with co-participation of the European Community fund FEDER (Project No. POCI/QUI/56569/2004).

Supporting Information Available: NOESY experiments of $(H_4[26]phen_2N_4O_2)^{4+}$ with btc^{3-} and iph^{2-} at pD 5 in D_2O at room temperature, and the crystallographic information for compounds **1** and **2**. Table S1 lists the hydrogen bonds, and Table S2 summarizes the crystal data together with refinement details. Table S3 presents a comparison of the association constants (log K_{eff}) of $[26]phen_2N_4O_2$ and other related receptors (available in literature) with selected anions at pH = 7.0. This material is available free of charge via the Internet at http://pubs.acs.org.

JO062653P